STRIP INTEGRATION IN RADIO ASTRONOMY

By R. N. Bracewell*

[*Manuscript received January* 17, 1956]

Summary

When a celestial source of radio waves is scanned with an aerial beam which is much longer than the source in one direction but suitably narrow in the other, the transformation from the true distribution to the measured value is referred to as strip integration. It is here treated as a special case of two-dimensional aerial smoothing in which the aerial beam is allowed to spin about its centre as it moves about the sky. It is shown that the resolution obtainable is set by the cross-sectional profile of the strip beam in the narrow dimension. Thus, when the strip reduces to a line, the resolution is complete and full reconstruction of the true distribution is possible; but scans must be made in all directions. In the general case it is shown that there is a principal solution, and that a finite number of scans suffices to determine it. A method is presented for reconstructing the principal solution from the observed data.

I. Introduction

When radio-astronomical observations are made with a fan beam, that is, with one which is long and narrow, the measured quantity is a weighted mean over that part of the celestial brightness distribution lying in the beam. We shall say that the true distribution has been subjected to two-dimensional aerial smoothing by the observational procedure, and it is our purpose to examine the possibilities of recovering the true distribution from the observations in the limiting case where the length of the fan beam greatly exceeds the extent of the source distribution. This special kind of two-dimensional aerial smoothing will be called strip integration. The problem is essentially the same problem of aerial smoothing which has been discussed by Bracewell and Roberts (1954) and by Bracewell (1956) in two papers which will be referred to subsequently as paper I and paper II. However, it is convenient to treat strip integration separately for two reasons. Firstly, strip integration gives not only the blurring effect of averaging over the immediate neighbourhood, but the more serious effect of confusion with distant parts of a source which happen to lie in the long strip. Secondly, when a survey is made with a beam which is circularly symmetrical, no extra information is obtained by rotating the aerial about its main axis. But a fan beam, and particularly a very long fan beam, yields different measurements in different position angles. This property has not yet been utilized in practice with only moderately elongated fan beams, but it is the essence of observations made with the very long fan beams discussed in this paper.

Strip integration has been encountered in a number of recently reported researches, and handled in ways described below, but so far no generally satis-

* Division of Radiophysics, C.S.I.R.O., University Grounds, Sydney; present address: Radio Propagation Laboratory, Stamford University, Stamford, California.

factory method of inverting the process has been proposed. Wild and Smerd in an interesting theoretical paper presented to the Radio Astronomy Symposium at Jodrell Bank in August 1955, have discussed the relation of a solution, assuming one can be obtained, to the true distribution. Covington and Broten (1954) have used a fan beam $0\cdot12\times22\cdot5°$ lying in the meridian to sweep over the Sun, and have unravelled the strip-integrated solar distribution by an approximate procedure leading to a circularly symmetrical distribution satisfying the observations within the limits of error. They did not deal with the non-symmetrical case nor establish the uniqueness of their solution.

Similar observations by Christiansen and Warburton (1953, 1955) using a fan beam $0\cdot05\times5°$ were carried out so as to sweep over the Sun in different position angles, and they have shown that the distributions along the polar and equatorial diameters are different. They have thus had to face the general problem of no circular symmetry.

The interferometric attempts to get the brightness distribution over the Sun have proceeded similarly from the observations of Stanier (1950) made in a single position angle and reduced on the assumption of circular symmetry, to those of O'Brien (1953) made in many position angles. Machin (1951) advanced the theoretical aspect of Stanier's reduction problem by demonstrating that the desired solution was the Hankel transform of the extrapolated data, and subsequently O'Brien's problem also yielded its solution as the two-dimensional Fourier transform of the extrapolated data (suitably presented). Christiansen and Warburton were able to utilize this work by calculating, by Fourier analysis of their data, what they would have observed had they used a two-aerial interferometer instead of their long array; then the procedure described by O'Brien could be applied. It is a curious fact that this procedure, which removes the effect of strip integration, itself involves further application, numerically, of the same operation (though along a line instead of a strip).

Line integration, which is the limiting case of strip integration as the width of the strip approaches zero, may be expressed as an integral transform as follows :

$$f_L(R,\theta)=\int_{-\infty}^{\infty}\int_{-\infty}^{\infty}f(x,y)\delta(x\cos\theta+y\sin\theta-R)\mathrm{d}x\mathrm{d}y, \qquad \ldots\ldots \quad (1)$$

where $f_L(R,\theta)$ is the result of line integrating $f(x,y)$ along the line AB (Fig. 1). It is customary to think of $f_L(R,\theta)$ as a function of the continuous variable R for various discrete values of θ, because of the observational method of keeping θ fixed as R varies, that is, of scanning the line AB through positions such as $A'B'$.

The problem now is, given f_L, to find f. If we have f_L for $\theta=\theta_1$ only, an important case because it often arises, the problem is not soluble : for if $f_1(x,y)$ satisfies equation (1) when $\theta=\theta_1$, so also does $f_1(x,y)+f_2(x,y)$, where, using an expression introduced in paper I, $f_2(x,y)$ is an " invisible distribution ", that is, one such that

$$\int_{-\infty}^{\infty}\int_{-\infty}^{\infty}f_2(x,y)\delta(x\cos\theta_1+y\sin\theta_1-R)\mathrm{d}x\mathrm{d}y=0. \qquad \ldots\ldots \quad (2)$$

If, however, in addition to $f_L(R,\theta_1)$ we have other information about the source distribution, then further progress may be made. For example, if it is known that the source has circular symmetry then the problem may be fully solved, as explained in Section II. Normally more scans than one will be needed and it has been a matter for discussion how many would suffice to determine a general distribution. Two scans at right angles have been thought enough. Three scans suffice if the source has the kind of elliptical symmetry described by Mills (1953) but as many as six (O'Brien 1953) or eight (Christiansen and Warburton 1953) have been deemed necessary in other cases. It is shown in Section III that scans in *all* directions are needed to solve equation (1) for $f(x,y)$. Moreover, given $f_L(R,\theta)$ for all R and θ, $f(x,y)$ is uniquely determined, since there are no invisible distributions, that is, only $f_2(x,y)\equiv 0$ can satisfy equation (2) for all θ. However, a finite number of scans suffices in the case of strip integration.

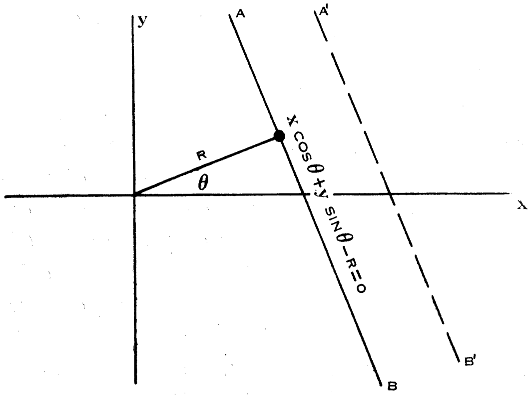

Fig. 1.—Illustrating line integration.

Strip integration, where the line is opened out into a strip with a profile given by the function $A(x)$, is expressed by an integral transform similar to equation (1), namely,

$$f_S(R,\theta)=\int_{-\infty}^{\infty}\int_{-\infty}^{\infty} f(x,y)A(x\cos\theta+y\sin\theta-R)\mathrm{d}x\mathrm{d}y, \quad \ldots . \quad (3)$$

where $f_S(R,\theta)$ is the result of strip integrating $f(x,y)$. The problem of finding $f(x,y)$ given $f_S(R,\theta)$ is more general than the previous one. We expect from paper I to encounter invisible distributions, that is, distributions satisfying

$$\int_{-\infty}^{\infty}\int_{-\infty}^{\infty} f(x,y)A(x\cos\theta+y\sin\theta-R)\mathrm{d}x\mathrm{d}y=0, \quad \ldots . \quad (4)$$

which will render the solution to equation (3) non-unique. However, a " principal solution " can be defined. We also find properties resembling the discrete-interval theorems of papers I and II, which facilitate computing and guide observations.

Among the questions discussed in Section IV are two of current practical importance in reducing observational data: (1) should the scans $f_S(R,\theta_i)$ be restored before proceeding to the solution or should one proceed straight to a solution and consider restoration in two dimensions? (2) Is there a method, resembling the method of successive substitutions, which will allow approximate solutions to be corrected?

II. Line Integration when there is Circular Symmetry

In general one is not concerned with sources which show circular symmetry, but, if they do, then one scan leads to a result; and often only one scan is available. This has been so in the early stages of several investigations in radio astronomy, for example, those of Covington, Stanier, and Christiansen and Warburton. Furthermore the same equation arises in another connexion in radio astronomy where a distant spherically symmetrical distribution is integrated along lines of sight (Bolton and Westfold 1951). Other reasons for studying this case before proceeding to the general problem, are that the numerical method of solution proposed here (1) leads to the method later proposed for the general problem and (2) is itself needed in dealing with the symmetrical component of a general distribution.

Let the brightness temperature distribution $f(x,y)$ depend only on r, where $r^2=x^2+y^2$, and let it be written $f(r)$. Then the line integrated distribution $f_L(R,\theta)$, given by equation (**1**), will be the same for all θ. Put $\theta=0$ in equation (**1**) and write $f_L(x)$ for $f_L(R,0)$. Then

$$f_L(x)=\int_{-\infty}^{\infty}\int_{-\infty}^{\infty} f(r)\delta(x-R)\mathrm{d}x\mathrm{d}y,$$

$$=2\int_{r=x}^{\infty} f(r)\mathrm{d}y,$$

or

$$f_L(x)=2\int_{x}^{\infty}\frac{f(r)r\mathrm{d}r}{(r^2-x^2)^{\frac{1}{2}}}. \qquad (5)$$

This is a form of Abel's integral equation and for convenience we may refer to $f_L(x)$ as the Abel transform of $f(r)$. An explicit solution for $f(r)$ may be found by converting the integral into a convolution integral. Put $\xi=x^2$ and $\rho=r^2$, and let $f_L(x)=F_L(x^2)$, $f(r)=F(r^2)$. Then equation (**5**) is replaced by

$$F_L(\xi)=\int_{-\infty}^{\infty} K(\xi-\rho)F(\rho)\mathrm{d}\rho,$$

or

$$F_L=K*F, \qquad (6)$$

where

$$K(\xi)=\begin{cases}(-\xi)^{-\frac{1}{2}} & (\xi<0),\\ 0 & (\xi\geqslant 0).\end{cases}$$

Equation (6) may be solved by taking the Laplace transform of both sides, solving the resulting algebraic equation for the transform of F, and retransforming. Then

$$F=-\frac{1}{\pi}K*F_L', \qquad (7)$$

or, alternatively, by a different choice of the factors of the transform of F,

$$F=\frac{2}{\pi}K^{-1}*F_L'', \qquad (8)$$

a solution which may also be obtained directly from equation (7) by integrating by parts. The solution is unique and there are therefore no invisible distributions (other than null functions). Reverting to f and f_L, we may write equations (7) and (8) as

$$f(r)=-\frac{1}{\pi}\int_r^\infty \frac{f_L'(x)\mathrm{d}x}{(x^2-r^2)^{\frac{1}{2}}}=-\frac{1}{\pi}\int_r^\infty (x^2-r^2)^{\frac{1}{2}}\frac{\mathrm{d}}{\mathrm{d}x}\left\{\frac{f_L'(x)}{x}\right\}\mathrm{d}x,$$

or, if the integrand is zero beyond $x=r_0$, and allowing for the possibility that the integrand may behave impulsively at r_0,

$$f(r)=-\frac{1}{\pi}\int_r^{r_0} \frac{f_L'(x)\mathrm{d}x}{(x^2-r^2)^{\frac{1}{2}}}+\frac{f_L(r_0)}{\pi(r_0^2-r^2)^{\frac{1}{2}}},$$

$$=\frac{1}{\pi}\int_r^{r_0} (x^2-r^2)^{\frac{1}{2}}\frac{\mathrm{d}}{\mathrm{d}x}\left\{\frac{f_L'(x)}{x}\right\}\mathrm{d}x-\frac{f_L'(r_0)}{\pi r_0}(r_0^2-r^2)^{\frac{1}{2}}.$$

The following table of Abel transforms was worked out from the formulae. In the first eight examples f and f_L are zero for r and x greater than a.

These results are illustrated in Figure 2 which also has graphs of F and F_L. A useful relation for checking Abel transforms is

$$\int_{-\infty}^\infty f_L(x)\mathrm{d}x=2\pi\int_0^\infty f(r)r\mathrm{d}r\,;$$

also

$$f_L(0)=2\int_0^\infty f(r)\mathrm{d}r.$$

Another property is that

$$K*K*F'=-\pi F, \qquad (9)$$

that is, the operation $K*$ applied twice in succession annuls differentiation; thus $K*$ is, in this sense, half-order integration. Conversely, F is the half-order differential coefficient of F_L. Fractional order differentiation has been extensively studied since a publication by Laplace in 1812 (e.g. see Doetsch 1943, p. 298), and as a result of its application to electric circuit problems by Heaviside (1922), is well known in modern circuit analysis (see e.g. Bush 1937 ; Starr 1953).

In our notation equation (9) is easily derived, for if $F_L = K*F$ implies $F = -\pi^{-1}K*F_L'$, then it follows further that $F_L' = K*F'$; whence

$$K*K*F' = K*F_L' = -\pi F.$$

When it becomes necessary to perform line integration numerically, advantage may be taken of the possibility of expressing equation (5) in terms of the convolution $K*F$. Approximate evaluation of $K*F$ by taking sums of products of $K(\rho)$ and $K(\xi-\rho)$ at discrete intervals of ρ is then facilitated by the fact that the numerical values of K are the same for all ξ. Furthermore

TABLE 1

ABEL TRANSFORMS

$f(r)$		$f_L(x)$	
Disk	1	Semi-ellipse	$2(a^2-x^2)^{\frac{1}{2}}$
	$(a^2-r^2)^{-\frac{1}{2}}$	Rectangle	π
Hemisphere	$(a^2-r^2)^{\frac{1}{2}}$	Parabola	$\frac{1}{2}\pi(a^2-x^2)$
Paraboloid	a^2-r^2		$\frac{4}{3}(a^2-x^2)^{3/2}$
	$(a^2-r^2)^{3/2}$		$\frac{3\pi}{8}(a^2-x^2)^2$
Cone	$a-r$		$a(a^2-x^2)^{\frac{1}{2}}-x^2\cosh^{-1}\frac{a}{x}$
	$\frac{1}{\pi}\cosh^{-1}\frac{a}{r}$	Triangle	$a-x$
	$\delta(r-a)$		$2a(a^2-x^2)^{-\frac{1}{2}}$
Gaussian	e^{-r^2/σ^2}	Gaussian	$\sigma\pi^{\frac{1}{2}}e^{-x^2/\sigma^2}$
	$r^2e^{-r^2/\sigma^2}$		$\sigma\pi^{\frac{1}{2}}(x^2+\frac{1}{2}\sigma^2)e^{-x^2/\sigma^2}$
	$\frac{r^2-\frac{1}{2}\sigma^2}{\sigma\pi^{\frac{1}{2}}}e^{-r^2/\sigma^2}$		$x^2e^{-x^2/\sigma^2}$
	$(b^2+r^2)^{-1}$		$\pi(b^2+x^2)^{-\frac{1}{2}}$
	$J_0(\omega r)$		$\frac{2}{\omega}\cos\omega x$
	$M\left(\frac{\omega r}{\pi}\right)$		$\frac{\sin^2\omega x}{\omega^2x^2}$

the values are the same, however fine an interval is chosen, save for a normalizing factor. Consequently a universal table of values can be set up for permanent reference. Table 2 shows coefficients for immediate use with values of F read off at $\rho=\frac{1}{2}, 1\frac{1}{2}, \ldots, 9\frac{1}{2}$, the scale of ρ being such that F becomes zero or negligible at $\rho=10$. The table gives mean values of K over the intervals 0–1, 1–2, . . . Thus at $\rho=n+\frac{1}{2}$ the value is

$$\int_n^{n+1} K(-\rho)\,d\rho = 2(n+1)^{\frac{1}{2}} - 2n^{\frac{1}{2}}.$$

Where N points of subdivision are used, the scale of ρ is arranged so that F becomes zero at $\rho=N$ and the coefficients are all multiplied by $(10/N)^{\frac{1}{2}}$.

As an example consider $F(\rho)=(10-\rho)^{\frac{1}{2}}$, for which the solution is known to be $F_L(\xi)=\frac{1}{2}\pi(10-\xi)$. We work at unit intervals of ρ, and copy the coefficients on a movable strip. The calculation in progress is shown in Table 3. The movable strip is in position for calculating $F_L(\xi)$ as the sum of products of corresponding values of F and K $(7\cdot78=2\cdot12\times2\cdot000+1\cdot87\times0\cdot828+\ldots$

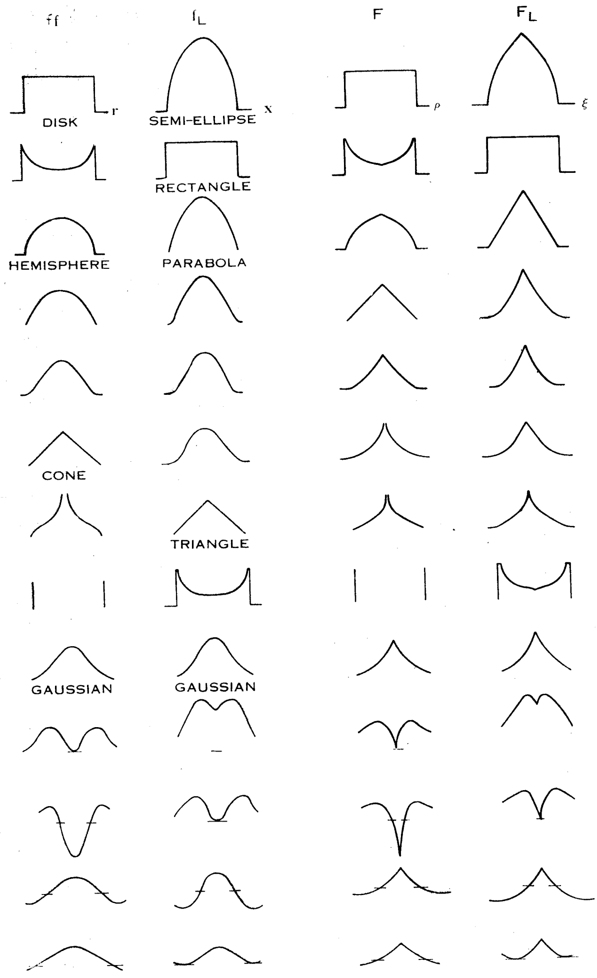

Fig. 2.—Some Abel transforms.

$+0\cdot71\times0\cdot472)$. This method for calculating Abel transforms numerically is very quick.

To perform the inverse operation, however, is the problem facing us; i.e. given F_L, to find F. We have equation (7) which leads directly to a solution if F_L is first differentiated. But if Table 3 is studied it will be perceived that the calculation just described can be done in reverse, using the values of F_L and working the movable strip upwards from the bottom. The strip is shown in position for calculating $F(5\frac{1}{2})$, let us say on a hand calculating machine. Form the products $0\cdot71\times0\cdot472, \ldots, 1\cdot87\times0\cdot828$, allowing them to accumulate in the product register. Clear the multiplier register, set 2·000 on the setting

TABLE 2

COEFFICIENTS FOR PERFORMING OR INVERTING THE ABEL TRANSFORMATION

ρ	K	ρ	K	ρ	K	ρ	K
$\frac{1}{2}$	2·000	$5\frac{1}{2}$	0·427	$10\frac{1}{2}$	0·309	$15\frac{1}{2}$	0·254
$1\frac{1}{2}$	0·828	$6\frac{1}{2}$	0·393	$11\frac{1}{2}$	0·295	$16\frac{1}{2}$	0·246
$2\frac{1}{2}$	0·636	$7\frac{1}{2}$	0·364	$12\frac{1}{2}$	0·283	$17\frac{1}{2}$	0·239
$3\frac{1}{2}$	0·536	$8\frac{1}{2}$	0·343	$13\frac{1}{2}$	0·272	$18\frac{1}{2}$	0·233
$4\frac{1}{2}$	0·472	$9\frac{1}{2}$	0·325	$14\frac{1}{2}$	0·263	$19\frac{1}{2}$	0·226

levers, and turn until 7·78 shows in the product register. The value $F(5\frac{1}{2})=2\cdot12$ then shows in the multiplier register. The inverse transformation performed in this way is practically as quick as the direct transformation.

TABLE 3

CALCULATING ABEL TRANSFORMS

ρ	F	K	F_L
			15·65
	3·08		
1			14·08
	2·91		
2			12·52
	2·74		
3			10·94
	2·55		
4			9·37
	2·35		
5		→	7·78
	2·12	2·000	
6			6·20
	1·87	0·828	
7			4·62
	1·58	0·636	
8			3·03
	1·22	0·536	
9			1·42
	0·71	0·472	
10			0
		0·427	
		....	

It is hardly necessary to point out that $f_L(x)$ depends only on values of $f(r)$ for which $r \geqslant x$. When we are given $f_L(x)$ for all x and we know $f(r)$ over an outer annulus (shown shaded in Fig. 3) then the value of $f(r)$ just inside the known region can be deduced from the integral along AB. This in effect is what the calculation does, and the graphical interpretation of it suggests a way of handling the problem when there is no circular symmetry.

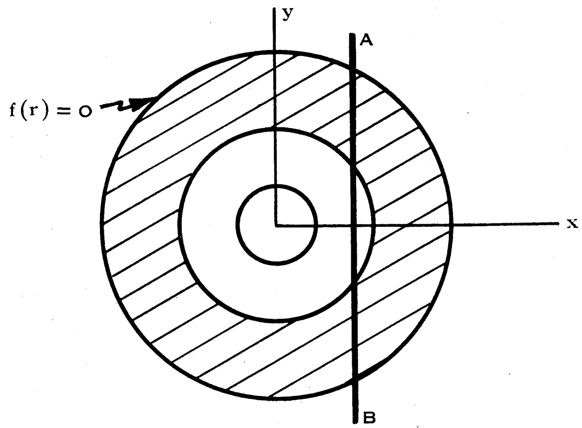

Fig. 3.—Contour diagram of $f(r)$ in the xy-plane.

III. Line Integration in the Absence of Symmetry

In this section we deal frequently with the following transforms which are therefore defined here for reference.

Fourier transform : $$\bar{f}(s)=\int_{-\infty}^{\infty}\mathrm{e}^{\mathrm{i}2\pi sx}f(x)\mathrm{d}x, \qquad \bar{f}=\mathbf{F}f. \quad \ldots (10)$$

Two-dimensional Fourier transform : $$\bar{f}(u,v)=\int_{-\infty}^{\infty}\int_{-\infty}^{\infty}f(x,y)\mathrm{e}^{\mathrm{i}2\pi(ux+vy)}\mathrm{d}x\mathrm{d}y, \quad \bar{f}={}^{2}\mathbf{F}f. \quad \ldots (11)$$

Hankel transform of zero order : $$f_H(\rho)=2\pi\int_{0}^{\infty}f(r)r\mathrm{J}_0(2\pi\rho r)\mathrm{d}r, \qquad f_H=\mathbf{H}f. \quad \ldots (12)$$

Abel transform : $$f_L(s)=2\int_{s}^{\infty}\frac{f(x)x\mathrm{d}x}{(x^2-s^2)^{\frac{1}{2}}}, \qquad f_L=\mathbf{A}f. \quad \ldots (13)$$

A great gain in clarity can be had in some places by the use of the abbreviated notation in terms of functional operators, shown on the right. The Abel transform has been discussed in Section II, but a note on the two-dimensional Fourier transform, the Hankel transform, and their relationship might be useful. Two-dimensional Fourier analysis decomposes a function of x and y into wave components such as that shown in Figure 4. Each such component is represented in amplitude and phase by a complex number on the uv-plane at a point whose polar coordinates (R,θ) represent respectively the wave number and the direction of the wave normal. When the function of x and y is circularly symmetrical, so also will its two-dimensional Fourier transform be, that is, both the function and its transform are functions of one (radial) variable only. On expressing this fact in equation (**11**) and integrating over the angular coordinate we find that the relationship between the two functions of radius only is equation (**12**). Thus if two circularly symmetrical functions are two-dimensional Fourier transforms, one of the other, then their cross-sectional profiles are Hankel transforms, one of the other.

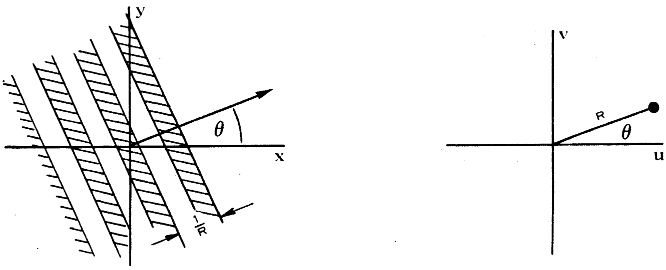

Fig. 4.—A two-dimensional Fourier component and its representation on the uv-plane.

The Hankel transformation is reciprocal, that is, $f_H = \mathbf{H}f$ and $f = \mathbf{H}f_H$, or $\mathbf{HH}f = f$, or

$$\mathbf{HH} = \mathbf{I},$$

where $\mathbf{I}$ is the operator which leaves a function unchanged. The operators $\mathbf{F}$ and $^2\mathbf{F}$ are not quite reciprocal but we may nevertheless write

$$\mathbf{FF} = {}^2\mathbf{F}{}^2\mathbf{F} = \mathbf{I},$$

if the i in equations (**10**) and (**11**) is changed to —i before repeating the operation. The operator $\mathbf{A}$ is not reciprocal and if applied twice is equivalent to integration (with respect to the proper variable as follows from Section II):

$$-\pi^{-1}\frac{\mathrm{d}}{\mathrm{d}(x^2)}\mathbf{AA} = \mathbf{I}.$$

Having noted these properties of the various transforms we can proceed to express line integration in terms of them. Let $f(x,y)$ be a true distribution of brightness temperature, as indicated roughly in Figure 5 by contours. The line integral $f_L(R,\theta)$ is given by equation (**1**) in which we shall put $\theta = 0$. Let $f_L(x) = f_L(R,0)$. Then $f_L(x)$, also shown in Figure 5, is the result of line integrating $f(x,y)$ along lines x=constant. Thus

$$f_L(x) = \int_{-\infty}^{\infty} f(x,y)\mathrm{d}y.$$

Consider now the Fourier transform of $f_L(x)$.

$$\begin{aligned}\mathbf{F}f_L &= \int_{-\infty}^{\infty} e^{i2\pi ux}\mathrm{d}x\int_{-\infty}^{\infty} f(x,y)\mathrm{d}y = \int_{-\infty}^{\infty}\int_{-\infty}^{\infty} e^{i2\pi ux}f(x,y)\mathrm{d}x\mathrm{d}y \\ &= \bar{f}(u,0),\end{aligned}$$

where $\bar{f}(u,v)$ is $^2\mathrm{F}f$. If now the contour diagram in the lower right-hand corner of Figure 5 stands for $\bar{f}(u,v)$, then $\bar{f}(u,0)$, the Fourier transform of $f_L(x)$, is the cross section along $v=0$. This cross section is shown rabatted into the uv-plane and cross hatched.

The result of line integrating at a different value of θ, for example along lines parallel to OP, is shown at the left on tilted axes. The Fourier transform of this curve is the cross section of $\bar{f}(u,v)$ along QR. We have now demonstrated the relationship of line integration to the Fourier transformation, and we can use this relationship to reach some immediate conclusions.

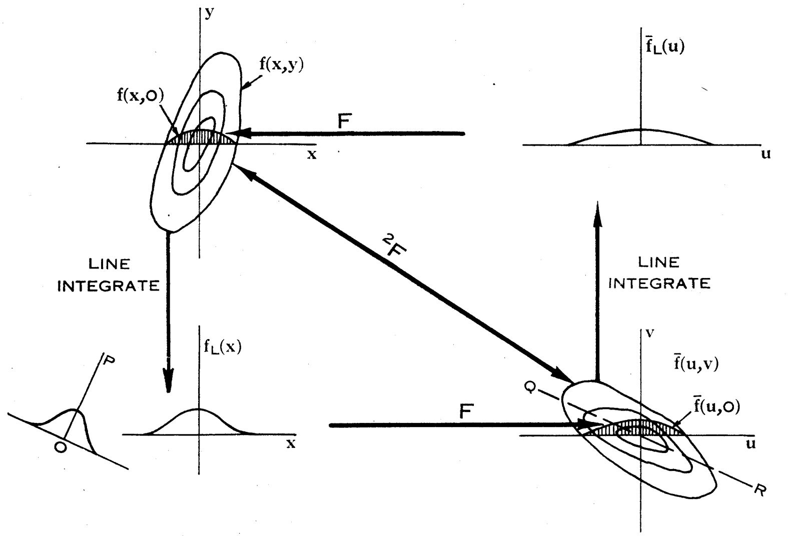

Fig. 5.—Synoptic chart of the relationship of line integration to one- and two-dimensional Fourier transforms.

Because of the uniqueness with which a function is defined by its Fourier transform it is clear that line integration for *all* θ is necessary to determine *every* cross section of $\bar{f}(u,v)$, without which $f(x,y)$ will not be determined. Hence all scanning directions must be used in order to find $f(x,y)$ from $f_L(R,\theta)$. Furthermore, when this is done, $f(x,y)$ is determined uniquely. Thus there can be no invisible distributions, in the non-symmetrical as in the symmetrical case.

Studies made with a two-aerial interferometer, whose beam pattern on the xy-plane is as in Figure 4, start with measurements of $\bar{f}(u,v)$ as the basic data. To find $f(x,y)$ it is necessary to take the two-dimensional Fourier transform. This one can do by line integrating and taking one-dimensional Fourier transforms, that is, by taking the path from $\bar{f}$ to f via $\bar{f}_L$ in Figure 5. Alternatively one might take Fourier transforms and perform the operation inverse to line integration, that is, proceed via f_L. The former procedure was introduced into radio astronomy by O'Brien (1953). By assembling all the different steps into the one diagram we obtain a convenient summary of the situation.

When $f(x,y)$ is circularly symmetrical we find further connexions among the operations, which are applicable not only to symmetrical sources but to symmetrical aerial patterns and to observational procedures which are symmetrical.

In the first place, line integration becomes Abel transformation. Then the cross sections of $f(x,y)$ and $\bar{f}(u,v)$, being independent of θ, become Hankel

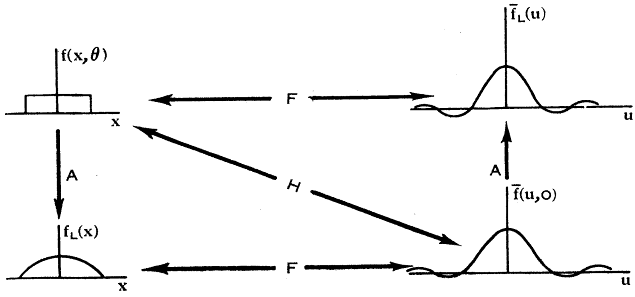

Fig. 6.—Relationships between the Fourier, Abel, and Hankel transformations.

transforms. Figure 6 summarizes this situation. The basic theorem brought out by this discussion is*

$$\mathbf{HFA}=\mathbf{I},$$

or

$$\int_0^\infty \mathrm{d}r J_0(2\pi\xi r)r\int_{-\infty}^\infty \mathrm{d}s e^{i2\pi rs}\int_s^\infty \frac{\mathrm{d}x2xf(x)}{(x^2-s^2)^{\frac{1}{2}}}=f(\xi).$$

Several other corollaries can be written down at sight.

$$\mathbf{HFA}=\mathbf{FAH}=\mathbf{AHF}=\mathbf{I},$$
$$\mathbf{H}=\mathbf{FA}\quad \mathbf{F}=\mathbf{AH}\quad \mathbf{A}=\mathbf{FH},$$
$$\mathbf{AFAF}=\mathbf{FAFA}=\mathbf{I},$$
$$\mathbf{AFA}=\mathbf{F},\quad \mathbf{A}=\mathbf{FA}^{-1}\mathbf{F}.$$

Some of these may be expressed in words as follows. The Fourier transform of the Abel transform is the Hankel transform. Abel transformation in the function domain corresponds to inverse Abel transformation in the Fourier transform domain. Table 4 gives four cyclical sets of functions related as in Figure 6, which itself illustrates the first set of functions in the table. The functions have been chosen because of their tendency to occur in the present work; thus the table summarizes four Hankel, seven Fourier, and eight Abel transform pairs.

How to perform the operation inverse to line integration, which may be referred to as reconstruction, may now be considered. Clearly one way of proceeding from f_L to f is via $\bar{f}$ and $\bar{f}_L$. Figure 7 summarizes what one must do, namely, (i) take Fourier transforms of all the line integrated profiles f_L,

* The compound operator **HFA** has the effect of applying the operations **A**, **F**, **H** in that order, i.e. $\mathbf{HFA}f=\mathbf{H}[\mathbf{F}(\mathbf{A}f)]$.

(ii) assemble the transforms into a two-dimensional function $\bar{f}$, (iii) line integrate $\bar{f}$ for all directions, (iv) take Fourier transforms of all the line-integrated profiles $\bar{f}_L$, and (v) assemble the transforms into the two-dimensional solution f. We shall refer to this as reconstruction by the roundabout path.

Direct reconstruction can be effected, in the case of circular symmetry, by a numerical method which is equivalent to the graphical method of Figure 3, and by a simple extension this method can be made applicable in the absence of symmetry.

TABLE 4

FOURIER-ABEL-HANKEL SETS*

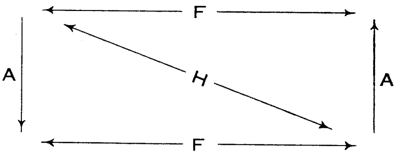

$\Pi\left(\frac{x}{2F}\right)$ $2(F^2-x^2)^{\frac{1}{2}}\Pi\left(\frac{x}{2F}\right)$	$\frac{\sin 2\pi F u}{\pi u}$ $\frac{F J_1(2\pi F u)}{u}$
$\frac{\sin 2\pi F x}{\pi x}$ $J_0(2\pi F x)$	$\Pi\left(\frac{u}{2F}\right)$ $\frac{1}{\pi(F^2-u^2)^{\frac{1}{2}}}$
$\frac{1}{2}\delta(x-F)$ $\frac{F}{(F^2-x^2)^{\frac{1}{2}}}$	$\cos 2\pi F u$ $\pi F J_0(2\pi F u)$
$M(Fx)$ $\frac{\sin^2 \pi F x}{\pi^2 x^2}$	$F(F^2-u^2)^{\frac{1}{2}}-u^2 \cosh^{-1}\frac{F}{u}$ $F\Lambda\left(\frac{u}{2F}\right)$

* In this table $\Pi(x)$ and $\Lambda(x)$ are respectively the rectangle and triangle functions of unit height and width, and $M(x)$ is defined in Section IV.

Let f be zero (or negligibly small) outside a closed contour C. Then starting from C one could work inwards proceeding at each step as explained in connexion with Figure 3. But C is not known; instead one knows that $f_L(R,\theta)$ is zero outside a curve L which may be seen to be the locus of the foot of the perpendicular from the origin on to those tangents to C which do not cut C. Given L one cannot determine C, but C will lie within, and largely coincide with, the envelope E of lines through the points of L perpendicular to the lines joining these points to the origin. The curve L is pedal to E, a relationship which was first pointed out in connexion with line integration by Dr. R. F. Mullaly.

Since points of C can lie outside neither E nor L, either of the latter may be made the starting boundary for reconstruction. Some points of technique facilitate the process. For example, it will often happen that there is approximate circular symmetry over a sector. Then in that sector the numerical procedure described earlier may be applied for some distance in. This method applies especially at the outer boundary where it may be used to get the process started. A coarse interval is suggested so that an approximate result can be obtained with the minimum computation ; then a test akin to that used in the method of successive substitutions can be applied to determine corrections. We now pause to consider application of the method of successive substitutions.

If φ is an approximation to f, then φ_L, which is obtained by line integrating φ, will be an approximation to f_L. Apply $f_L-\varphi_L$, suitably normalized, as a correction to φ at (R,θ) to give φ_1 as a new approximation which may then in its turn be corrected. Then the question is, do the successive approximations φ, φ_1, etc. tend to the solution f ? It can be shown that even for the case of circular

$$
\begin{tikzcd}
f \arrow[d, "\text{LINE INTEGRATE}"'] & \bar{f}_L \arrow[l, "F"'] \\
f_L \arrow[r, "F"'] & \bar{f} \arrow[u, "\text{LINE INTEGRATE}"']
\end{tikzcd}
$$

Fig. 7.—The inversion of line integration.

symmetry this is not in general so, and a modification has to be sought. A satisfactory outcome results if one incorporates the correction at each point before proceeding to correct the next, and if one works inwards in such a manner that at each step the value to be corrected is the only uncorrected value on the line of integration. The φ_1 so obtained must then be equal to f (to the order of accuracy permitted by the coarseness of the intervals).

Considerable work is involved in performing direct reconstruction as described above, but comparison with the only other known method is favourable; for reconstruction by the roundabout path involves precisely the same amount of line integration together with a large number of Fourier transformations and graphical manipulations. Attention to the detail of performing line integration is indicated, and in the next section it will be shown how line integration in radio astronomy can in practice be reduced exactly to a summation.

IV. Strip Integration

A diagram is useful for surveying the complexities of strip integration. It is clear, even without reference to equations (**1**) and (**3**), that the strip-integrated function $f_S(R,\theta)$ is related to $f_L(R,\theta)$ by convolution with the profile A of the aerial beam. Thus

$$f_S(R,\theta)=A(R)*f_L(R,\theta).$$

We may put $\theta=0$ and write $f_S(x)$ for $f_S(R,0)$. Figure 8 shows $f_S(x)$ on an extended diagram of the type of Figure 5. The Fourier transforms of $f_L(x)$ and $f_S(x)$, which are shown to the right, are related through multiplication by $\bar{A}$.

The profiles $f_S(x)$ are observed for different values of θ and it is then required to find $f(x,y)$.

Method I.—One may first restore the profiles $f_S(x)$ as in paper I or, preferably, by the chord construction (Bracewell 1955), and then reconstruct as in Section III.

Method II.—Alternatively, one might reconstruct first and then restore as in paper II, but the restoration would be two-dimensional and not as convenient. However, as the value of restoration is sometimes doubtful, it may in some cases be desirable to postpone considering restoration until after reconstruction. The question then arises how such restoration may be done.

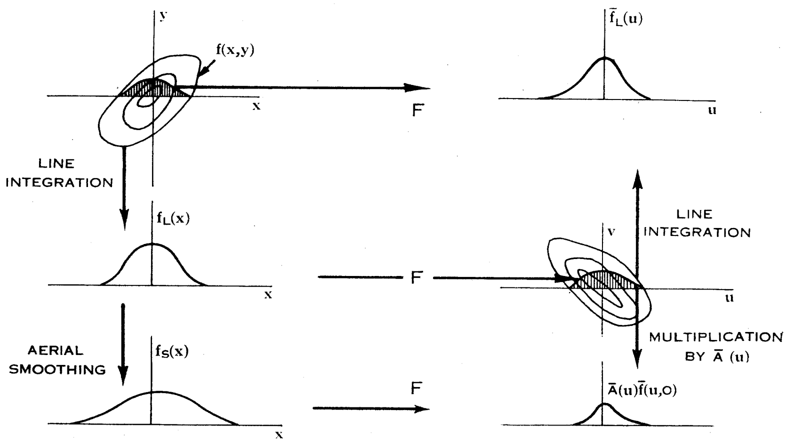

Fig. 8.—Strip integration considered as line integration followed by aerial smoothing.

Method III.—The only method so far applied has been as follows : (i) take Fourier transforms of all profiles $f_S(x)$, (ii) correct each transform for aerial smoothing by dividing by $\bar{A}$, (iii) assemble into a two-dimensional contour diagram, (iv) line integrate in all directions, (v) take Fourier transforms of all line-integrated profiles, (vi) assemble the transforms into a contour diagram representing the solution. As before, one might defer restoration until the end. The labour involved in this roundabout method is so great that it will probably fall into disuse now that a direct procedure is available.

The interesting question raised regarding the commutativity of restoration and reconstruction may now be studied. If a line-integrated profile $f_L(x)$ had a Fourier transform which cut out to zero at $u=u_c$, then the two-dimensional Fourier transform of $f(x,y)$ would fall to zero at $u=u_c$, $v=0$ (see Fig. 5). Now $f_S(x)$, which is derived from $f_L(x)$ by aerial smoothing, must have this property, and similarly for the strip-integrated profiles at all values of θ. The cut-off value of $\sqrt{(u^2+v^2)}$ will be the same for all θ ; hence the distribution over the uv-plane, of which $\bar{A}(u)\bar{f}(u,0)$ in Figure 8 is the $\theta=0$ cross section, must have a circular boundary and be zero outside. Call this function $\overline{\overline{F}}(u,v)$. Let the aerial pattern be given by

$$A(x)=\left(\frac{\sin \pi x u_c}{\pi x u_c}\right)^2.$$

Then

$$\bar{A}(u)=\Lambda\left(\frac{u}{2u_c}\right),$$

where $\Lambda(u)$ is the triangle function of unit height and base, that is,

$$\Lambda(u)=\begin{cases}1-2\mid u\mid & (\mid u\mid<\frac{1}{2})\\ 0 & (\mid u\mid>\frac{1}{2}).\end{cases}$$

Thus

$$\overline{\overline{F}}(u,v)=\Lambda\left\{\frac{\sqrt{(u^2+v^2)}}{2u_c}\right\}\bar{\bar{f}}(u,v).$$

If now one proceeds, without restoration, to reconstruct from $f_S(x)$, the result will be $F(x,y)$ instead of $f(x,y)$, where $F(x,y)$ is the two-dimensional Fourier transform of $\overline{\overline{F}}(u,v)$. By the two-dimensional convolution theorem

$$F=M*f,$$

where $M(Fr)$ is the Hankel transform of $\Lambda(\rho/2F)$:

$$M=\mathbf{H}\Lambda.$$

Consequently F differs from f through being smoothed with a pattern $M(Fr)$; hence f can be recovered as well by restoration following reconstruction as otherwise. This fact was demonstrated by Wild and Smerd.

From Table 4 we see that M may easily be calculated numerically as the inverse Abel transform of $\pi^{-2}x^{-2}\sin^2\pi Fx$, but the Hankel transform may in this case also be readily performed in terms of tabulated functions. Thus

$$\begin{aligned}M(Fr)&=2\pi\int_0^\infty \rho\Lambda\left(\frac{\rho}{2F}\right)\mathrm{J}_0(\rho r)\mathrm{d}\rho\\ &=2\pi\int_0^F \rho\left(1-\frac{\rho}{F}\right)\mathrm{J}_0(\rho r)\mathrm{d}\rho.\end{aligned}$$

After integration by parts, and with some reduction,

$$M(\zeta)=2\pi F^2\{\zeta^{-3}j(\zeta)-\zeta^{-2}\mathrm{J}_0(\zeta)\},$$

where $\zeta=Fr$ and

$$j(\zeta)=\int_0^\zeta \mathrm{J}_0(\zeta)\mathrm{d}\zeta,$$

a tabulated function.*

* See, for example, Watson (1944) or National Bureau of Standards (1954).

All the functions and operations involved in the above discussion can be summarized for reference by arranging them on the vertices and edges of a cube as in Figure 9 (*a*). Using the particular aerial pattern assumed above, we illustrate in Figure 9 (*b*), the four equivalent functions representative of the aerial, and the relations between them. This figure is taken from the last set of functions of Table 4. Figure 9 (*c*) shows how methods I, II, and III described above may be stated diagrammatically as paths on the cube. O'Brien's method is also indicated. On this diagram it is easy to see alternative paths from one point to another, and to study their significance. Some of the less obvious relationships so revealed might well prove useful in future deliberations.

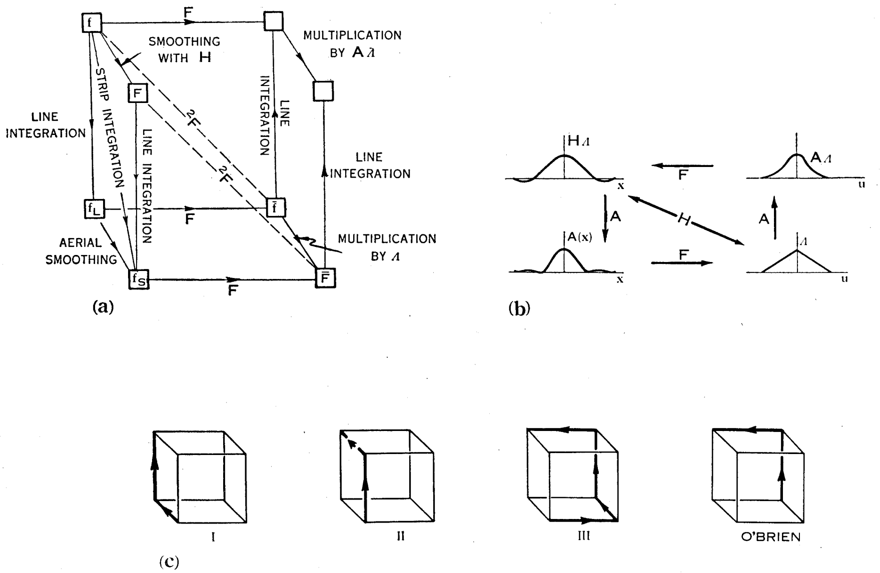

Fig. 9.—Relationships between functions involved in strip integration.

In Figure 9 (*a*) all four operations represented by lines parallel to that joining f_L to f_S are irreversible, since information is lost in the process. Therefore when in Figure 9 (*c*) we show arrows running in the reverse direction, for example from F to f, it is understood that one will not recover f itself but an approximation to f whose Fourier transform is zero outside a certain region.

We have seen how in principle to invert strip integration, and now prove a theorem which adds greatly to the practicability of the method.

If a function f(x) *has a Fourier transform* $\bar{\mathrm{f}}(\mathrm{s})$ *which is zero for* $\mathrm{s}>\tau_0^{-1}$, *then* $\int_{-\infty}^{\infty}\mathrm{f}(\mathrm{x})d\mathrm{x}$ *is equal to* τ *times the sum of values of* f(x) *separated by interval* τ, *where* τ *is any interval shorter than* τ_0. For

$$\int_{-\infty}^{\infty} f(x)\mathrm{d}x=\bar{f}(0)\,;$$

but

$$\tau \mathrm{III}(\tau s) * \bar{f}(s) = \bar{f}(s), \qquad s = 0,$$

provided $\tau < \tau_0$. Therefore, since the Fourier transform of $\tau \mathrm{III}(\tau s) * \bar{f}(s)$ is $\mathrm{III}(x/\tau) f(x)$,

$$\int_{-\infty}^{\infty} f(x) \mathrm{d}x = \int_{-\infty}^{\infty} \mathrm{III}\left(\frac{x}{\tau}\right) f(x) \mathrm{d}x = \tau \sum_{n=-\infty}^{\infty} f(x - n\tau).$$

As in papers I and II, the row-of-spikes function $\mathrm{III}(x)$ is defined by

$$\mathrm{III}(x) = \sum_{n=-\infty}^{\infty} \delta(x+n).$$

The interval τ_0 is twice the peculiar interval at which discrete values of $f(x)$ suffice to specify $f(x)$ and is therefore quite coarse: for $x^{-2} \sin^2 x$ we have $\tau_0 = \pi$ and for $x^{-1} \sin x$, $\tau_0 = 2\pi$. If one takes $\tau = \tau_0$ then the summation will be subject to a correcting factor $(1+D)^{-1}$ if there is an average discontinuous jump $D\bar{f}(0)$ in $\bar{f}(s)$ at $s = \pm \tau_0^{-1}$; in the case of $x^{-1} \sin x$, $D = 1$.

In line integrating a function $\varphi(x,y)$ in the course of reconstruction by method I, the integral is correctly evaluated by summing discrete values taken along the straight line at intervals which are equal to twice the peculiar interval of the aerial as defined in paper I. This follows from the theorem because in method I the line integrals are compared with points on strip-integrated profiles which are free from Fourier components of semi-period greater than the peculiar interval of the aerial.

The possibility of obtaining line integrals correctly by quite coarse summing is directly helpful, but has another implication which is no less important. Since only discrete information is utilized, scans in all directions are not required; only enough scans are wanted to permit the process of reconstruction. On this basis one can answer the question of how many position angles should be programmed for observation.

Let the units of x and y equal the peculiar interval associated with A and let the major diameter of the source be D. If N position angles, equally spaced between 0 and π are used, then, at the boundary of the source, observations will be spaced by at most $\frac{1}{2}\pi D/N$. This spacing must not exceed the spacing needed for the summation which gives the line integral. Hence

$$\pi D/2N \leqslant 2, \quad \text{or} \quad N \geqslant \pi D/4.$$

For example, if the diameter of the Sun is 20 peculiar intervals, at least 16 different position angles are necessary. In the case of symmetrical objects like the quiet Sun, the number of necessary directions is halved.

A final remark bearing on the practical details of inverting strip integration may be added. Since the Abel transformation may be so readily inverted, by the method of Section II, a symmetrical component may be worth subtracting from the data. If the unsymmetrical residual is small in comparison, then not such high accuracy is required in inverting the strip integration as when the whole is handled at once. In the author's opinion this method would be suitable in the case of the Sun.

V. Fan Beams

The typical fan beam is that produced by a rectangular array or rectangular aperture, and if the aperture distribution is uniform the aerial pattern is approximately of the form

$$\frac{\sin k_1 x}{x} \cdot \frac{\sin k_2 y}{y}.$$

When such a beam is displaced parallel to itself, the situation can be reduced approximately to that of a circular beam by working in terms of the peculiar interval appropriate to each of the x and y directions. But when the beam may rotate about its centre a new factor is introduced. More information is available since there are now three independent variables (x, y, and ψ) instead of two (x and y). The more elongated the beam the more the additional information, but on the other hand, the elongation itself means a reduction in information. It will now be shown that the gain and loss counterbalance each other exactly.

Consider a circularly symmetrical beam $A\{\sqrt{(x^2+y^2)}\}$ with Hankel transform $B\{\sqrt{(u^2+v^2)}\}$ which falls to zero where $\sqrt{(u^2+v^2)}=P$. From a survey of a distribution $f(x,y)$ with such a beam, $\bar{f}(u,v)$ can be recovered out to a distance P from $u=0$, $v=0$. Now let the beam be elongated by a factor b in the y direction. The new beam $A\{\sqrt{(x^2+b^{-2}y^2)}\}$ has a Hankel transform proportional to $B\{\sqrt{(u^2+b^2v^2)}\}$ and from a survey with such a beam less of $\bar{f}(u,v)$ is recoverable, but it is still recoverable out to a distance P in one direction. As the elongated beam is turned through all ψ, $\bar{f}(u,r)$ is recovered out to a distance P in all directions on the uv-plane. Hence as much information about $f(x,y)$ is obtainable by spinning the elongated beam as is yielded by the small circular beam.

If the elongated beam is produced by a rectangular array then it does not reduce exactly to a circularly symmetrical beam when contracted, so the situation is a little more complicated. It can be shown that the information obtained by spinning such a beam exceeds what is obtained with the small non-elongated beam which would be produced by stretching the rectangular array out into a square. But the difference is exactly compensated by the extra information available from the non-elongated beam itself, if it is spun.

Two special cases of this fan beam theorem yield earlier results of this paper. Let the fan beam be infinitely elongated into a strip beam. Then the cross-sectional profile determines the resolution. But this was the result we deduced for strip integration, and it will be seen that the doubly infinite ensemble of measurements made by strip scanning are exactly those made by surveying with a spinning strip beam. For the degeneracy of the strip beam reduces the three independent variables specifying the fan beam position to two. Likewise, when the fan beam is infinitely elongated one way, and infinitely narrow the other, our result shows that spinning the beam will give infinitely sharp resolution. But such a survey gives precisely the measurements obtained by line scanning, which, as known from Section III, uniquely determines the true distribution.

VI. References

Bolton, J. G., and Westfold, K. C. (1951).—*Aust. J. Sci. Res.* A **4**: 476.

Bracewell, R. N., and Roberts, J. A. (1954).—*Aust. J. Phys.* **7**: 615.

Bracewell, R. N. (1955).—*Aust. J. Phys.* **8**: 200.

Bracewell, R. N. (1956).—Two-dimensional aerial smoothing in radio astronomy. *Aust. J. Phys.* **9** (3) (in press).

Bush, V. (1937).—" Operational Circuit Analysis." (Wiley: New York.)

Christiansen, W. N., and Warburton, J. A. (1953).—*Aust. J. Phys.* **6**: 262.

Christiansen, W. N., and Warburton, J. A. (1955).—*Aust. J. Phys.* **8**: 474.

Covington, A. E., and Broten, N. W. (1954).—*Astrophys. J.* **119**: 569.

Doetsch, G. (1943).—" Theorie und Anwendung der Laplace-Transformation." p. 298. (Dover: New York.)

Heaviside, O. (1922).—" Electromagnetic Theory." (Benn: London.)

Machin, K. C. (1951).—*Nature* **167**: 889.

Mills, B. Y. (1953).—*Aust. J. Phys.* **6**: 452.

National Bureau of Standards (1954).—Tables of functions and zeros of functions. Appl. Math. Ser. No. 37.

O'Brien, P. A. (1953).—*Mon. Not. R. Astr. Soc.* **113**: 597.

Stanier, H. M. (1950).—*Nature* **165**: 354.

Starr, A. T. (1953).—" Radio and Radar Technique." (Pitman: London.)

Watson, G. N. (1944).—" Theory of Bessel Functions." 2nd Ed. (Cambridge Univ. Press.)